

University of Wisconsin - Madison

LBL-35746
MAD/PH/837
hep-ph@xxx/9406413
 June 1994

STRONG WW SCATTERING AT PHOTON LINEAR COLLIDERS*

M. S. Berger^a and M. S. Chanowitz^b

^a*Physics Department, University of Wisconsin
 Madison, WI 53706, USA*

^b*Lawrence Berkeley Laboratory
 Berkeley, CA 94720, USA*

ABSTRACT

We investigate the possibility of observing strong interactions of longitudinally polarized weak vector bosons in the process $\gamma\gamma \rightarrow ZZ$ at a photon linear collider. We make use of polarization of the photon beams and cuts on the decay products of the Z bosons to enhance the signal relative to the background of transversely polarized ZZ pairs. We find that the background overwhelms the signal unless there are strong resonant effects, as for instance from a technicolor analogue of the hadronic $f_2(1270)$ meson.

1. Introduction

Back-scattering of low energy laser photons from the beams of a high energy e^+e^- linear collider offers the possibility of obtaining photon-photon collisions of energy and luminosity comparable to that of the parent e^+e^- collider.[1] Here we consider whether such photon-photon colliders could be used to study a strongly interacting electroweak symmetry breaking sector in the process $\gamma\gamma \rightarrow Z_L Z_L$, where Z_L denotes a Z boson of longitudinal polarization. If the symmetry breaking sector is strongly interacting $\gamma\gamma \rightarrow Z_L Z_L$ is analogous to the hadronic process $\gamma\gamma \rightarrow \pi^0\pi^0$.

Other studies of this process have been reported previously.[2] Here we focus on whether the signal can be observed over the background from transversely polarized Z pairs, using strategies developed for the study of strong WW scattering at multi-TeV colliders. We conclude that nonresonant signals are probably not observable but that resonant signals, such as that of a tensor meson analogous to the hadron $f_2(1270)$, could be observable with integrated luminosity of order 100 fb^{-1} and energy near the production threshold. Nonresonant strong WW dynamics would be better observed at a photon linear collider in the processes[3] $\gamma\gamma \rightarrow WWW, ZZWW$, analogous to the strong scattering process[4] $qq \rightarrow qqWW$.

*Presented by MSB at the Workshop on Gamma-gamma Colliders, 28-31 March 1994, Berkeley, California.

The process $\gamma\gamma \rightarrow ZZ$ seems more promising than $\gamma\gamma \rightarrow W^+W^-$ which has a large tree-level background cross section of order 90 pb, of which even the $W_L^+W_L^-$ is dominated by the Born approximation near threshold. Since it vanishes in Born approximation, the process $\gamma\gamma \rightarrow ZZ$ is more promising. However Jikia has shown that the one loop contribution to $\gamma\gamma \rightarrow ZTZT$ is also quite large[5], large enough to overwhelm the Higgs boson signal in $\gamma\gamma \rightarrow H \rightarrow ZZ$ for $m_H > 400$ GeV. His calculation has now been confirmed both analytically[6] and numerically[7]. Strong scattering signals are likely to be even smaller, and we find that the $ZTZT$ background is over two orders of magnitude larger than the typical nonresonant $\gamma\gamma \rightarrow ZLZL$ signal. Drastic improvements must be found if the signal is to be observable.

2. Nonresonant Strong Scattering Signals and Background

The leading contribution to $\gamma\gamma \rightarrow ZZ$ occurs via $\gamma\gamma \rightarrow W^+W^-$ with rescattering of the final state into ZZ as for instance in Fig. 1. This is the dominant contribution both to the nonperturbative strong interaction $ZLZL$ signal and the perturbative $ZTZT$ background.

In the case of Higgs boson production, $\gamma\gamma \rightarrow H \rightarrow ZZ$, the signal cross section decreases with increasing mass m_H while in the threshold region the background ZZ cross section increases rapidly. At about $m_H > 400$ GeV the signal is overwhelmed by the background. In Higgs boson models the rise of the $W_L^+W_L^- \rightarrow ZLZL$ amplitude (the so-called “bad high energy behavior”) is cut off by the Higgs boson exchange amplitude at $\sqrt{s} = m_H$. In strong scattering models, as considered here, the cancellation is deferred to the ~ 2 TeV scale where the leading $J = 0$ partial wave amplitude saturates unitarity. This results in an excess of $ZLZL$ pairs from the uncancelled gauge sector $W_L^+W_L^- \rightarrow ZLZL$ amplitude that is the nonresonant strong scattering signal. The exact nature of the signal depends on strong interaction dynamics that is *a priori* unknown. We will illustrate the nonresonant strong scattering signal by using two models that when applied to QCD crudely represent, though underestimate, the experimental data for $\gamma\gamma \rightarrow \pi^0\pi^0$.

The signal-to-background ratio improves with increasing energy because the $ZTZT$ background becomes more strongly peaked in the forward and backward directions and so can be more efficiently removed by a cut on the scattering angle. Further gains are possible by using polarized photon beams chosen to favor the strong scattering signal over the background. For nonresonant strong scattering the $J = 0$ channel predominates at the energies under consideration and is enhanced by choosing photon beams of equal helicity, hence with total $J_Z = 0$. The tensor meson signal is favored by choosing opposite photon helicities that sum to $J_Z = 2$.

As shown previously for strong WW scattering at hadron colliders[8], the longitudinally polarized $ZLZL$ signal can be enhanced over the transversely polarized background at large \sqrt{s} by imposing a p_T cut on the decay products of the Z ’s. This discriminates against transversely polarized Z ’s because their decay products tend to be aligned along the Z boson line-of-flight, while the decay products of longitudinally polarized Z ’s are predominantly perpendicular to the Z line of flight.

(See Figure 2.) The normalized decay distributions are

$$\frac{1}{\Gamma} \frac{d\Gamma}{d \cos \theta^*} = \begin{cases} \frac{3}{4} \sin^2 \theta^* & \lambda_Z = L \\ \frac{3}{8} (1 + \cos^2 \theta^*) & T \end{cases} \quad (1)$$

where θ^* is the angle between the direction in the Z rest frame of the decaying quark or lepton and the direction of the Z in the lab. The decay product moving against the Z boson line-of-flight will tend to be soft and will often be rejected by the p_T cut. The larger \sqrt{s} , the more highly boosted are the Z bosons and the greater the effectiveness of the cut.

We consider the decay modes $ZZ \rightarrow q\bar{q}\nu\bar{\nu}$, $\ell^+\ell^-\nu\bar{\nu}$, $q\bar{q}\ell^+\ell^-$, and $\ell^+\ell^-\ell^+\ell^-$, which account for 40% of the Z pair decays. We do not consider the four jet final state because it is likely to be overwhelmed by the much larger four jet mode of the WW background, even given excellent jet-jet mass resolution. We ignore backgrounds from a Z boson going down the beam pipe or disappearing into a crack in the detector. The relevant variables are the transverse mass $M_{ZZ,T} = 2\sqrt{M_Z^2 + p_{T,Z}^2}$ (where $p_{T,Z}$ is the transverse momentum of the observed Z) and p_T , the smallest transverse momentum of an observable (i.e., not neutrino) Z decay product.

We use the following three cuts: (1) $|\cos \theta_{\text{lab}}| < \cos \theta_{\text{max}}$; (2) $M_{ZZ,T} > M_{ZZ,T}^{\min}$; (3) $p_T > p_T^{\min}$. For simplicity, in the $\sim 10\%$ of the events in which both Z 's can be reconstructed, $q\bar{q}\ell^+\ell^-$ and $\ell^+\ell^-\ell^+\ell^-$, we arbitrarily designate one of the Z 's as the “observable” one and proceed as above. This reduces the effectiveness of the cuts relative to what is actually attainable, especially the p_T cut, so that the results presented below err on the pessimistic side.

To exemplify nonresonant strong scattering we consider two models for $W_L^+ W_L^- \rightarrow ZZ_L$ scattering that smoothly extrapolate the threshold behavior required by the low energy theorems[4, 9] in a manner consistent with unitarity. The linear model extrapolates the *absolute value* of the $J = 0$ partial wave amplitude. Applied to $\pi^+\pi^- \rightarrow \pi^0\pi^0$ scattering it is

$$|a_0| = X \cdot \theta\left(\frac{2}{3} - X\right) + \frac{2}{3} \cdot \theta\left(X - \frac{2}{3}\right), \quad (2)$$

where $X = (s - m_\pi^2)/16\pi F_\pi^2$. The cross section is then[10, 11]

$$\sigma = \frac{\beta\alpha^2}{\pi s} |a_0|^2. \quad (3)$$

The factor 2/3 follows from decomposing $a_0(\pi^+\pi^- \rightarrow \pi^0\pi^0)$ into isospin channels a_{IJ} , that is, $a_0 = \frac{2}{3}(a_{00} - a_{20})$, and applying elastic unitarity to the a_{IJ} .

The second model uses the more gradual K-matrix unitarization,

$$a_{00} = X_0(1 - iX_0)^{-1}, \quad (4)$$

$$a_{20} = -X_2(1 + iX_2)^{-1}, \quad (5)$$

where $X_0 = (s - \frac{m_\pi^2}{2})/16\pi F_\pi^2$ and $X_2 = (s - 2m_\pi^2)/32\pi F_\pi^2$. The cross section for $\gamma\gamma \rightarrow \pi^0\pi^0$ is

$$\sigma = \frac{\beta\alpha^2}{\pi s} \left(\frac{2}{3}|a_{00} - a_{20}|\right)^2. \quad (6)$$

The models slightly underestimate the experimental data from the Crystal Ball[12] below 700 MeV as shown in Figure 3. We apply the models to $W_L^+W_L^- \rightarrow Z_L Z_L$ by setting $m_\pi = 0$ and taking $F_\pi \rightarrow v$. The conclusions given below would not change even if the amplitudes were increased by a factor of two.

We convolute the gamma-gamma cross sections with the luminosity distributions to obtain the total cross sections given in Tables 1 and 2, which do not include decay branching ratios. We consider two cases: (i) unpolarized beams and (ii) polarized photon and electron beams, $\lambda_\gamma = -1$ and $\lambda_e = 1/2$. In Tables 1 and 2 the strong scattering signal is less than 1 fb. Since the TT background is 260 fb, the signal is more than two orders of magnitude smaller than the background before any cuts are made.

The correlations between the final state fermions are obtained by using the decay density matrix ρ for each Z boson,

$$\sigma_{\lambda_1 \lambda_2} = \sum_{\lambda_3 \lambda'_3 \lambda_4 \lambda'_4} \int \mathcal{M}_{\lambda_1 \lambda_2 \lambda_3 \lambda_4} \mathcal{M}_{\lambda_1 \lambda_2 \lambda'_3 \lambda'_4}^* \rho_{\lambda_3 \lambda'_3} \rho_{\lambda_4 \lambda'_4} d\text{LIPS}. \quad (7)$$

The results are summarized in tables 3 and 4 where we exhibit the number of signal and background events for 100 fb^{-1} with fixed angle cut $\cos(\theta_{\text{lab}}) < 0.7$ and with the cuts on p_T and $M_{ZZ,T}$ chosen to optimize the statistical significance of the signal. We have investigated increasing the angle cut to $|\cos \theta_{\text{lab}}| < 0.6$ and find that this does not increase the statistical significance of the signal. The $S : B$ ratios are too small to be observable, even if the statistical significance S/\sqrt{B} were enhanced by imagining still higher luminosity.

3. Tensor Resonance

Far enough above threshold $J \neq 0$ partial waves begin to contribute to $\gamma\gamma \rightarrow Z_L Z_L$ scattering. Just as the d-wave begins to emerge in $\pi\pi$ scattering above 1 GeV, we might expect d-wave scattering in $\gamma\gamma \rightarrow Z_L Z_L$ to set in above about $v/F_\pi \cdot 1 \text{ GeV} \sim 2.5 \text{ TeV}$. In hadron physics the d-wave saturates unitarity at the peak of the $f_2(1270)$ resonance, which in $SU(3)_{TC}$ would correspond to $\sim 3.4 \text{ TeV}$. Figure 4 shows that the experimental cross section for $\gamma\gamma \rightarrow \pi^0 \pi^0$ is nearly two orders of magnitude larger than the nonresonant models at the peak of the f_2 and a few times larger in the region of the $f_0(975)$ scalar resonance.

To illustrate a resonant signal we use the experimental data for $\gamma\gamma \rightarrow f_2(1270) \rightarrow \pi^0 \pi^0$ with the energy rescaled by $v/F_\pi \sim 2700$, as expected in a technicolor theory with an $SU(3)$ gauge group. Using conventional large N scaling estimates we also consider the $SU(5)_{TC}$ technicolor gauge group which implies lower mass, and therefore more easily observable, techni-hadrons. The mass and width of the technitensor are then obtained from the hadron $f_2(1270)$,

$$M_{f_{TC}} = \sqrt{\frac{3}{N_{TC}}} \frac{v}{f_\pi} M_f, \quad (8)$$

$$\Gamma_{f_{TC}} = \frac{3}{N_{TC}} \frac{M_{f_{TC}}}{M_f} \Gamma_f. \quad (9)$$

We assume the peak at 1270 MeV in the data is comprised of the ratios $D_2:D_0:S=0.8:0.2:0$. That is we assume for simplicity that the peak has only a tensor component, despite the fact that there is evidence for a $J = 0$ component. Since the helicity of the QCD tensor is predominantly $J_Z = 2$, unpolarized beams are preferable to the polarized beams used for the s-wave contributions. Polarization settings that isolate the $J_Z = 2$ helicity, may improve the situation beyond that obtained with unpolarized beams.

The signal (for $N_{TC} = 3$) and background are displayed in Fig. 5 for unpolarized beams at a $\sqrt{s_{e^+e^-}} = 4$ TeV collider (which has maximum $\gamma\gamma$ energy $\sqrt{s_{\gamma\gamma}} \sim 3.2$ TeV). The signal is smaller than it would be for $N_{TC} > 3$ because the peak is partially beyond the reach of the $\gamma\gamma$ center-of-mass energy. The statistical significance of the signal is maximized with a transverse mass cut $M_{ZZ,T} > 2800$ GeV. With 100 fb^{-1} of integrated luminosity this yields 28.6 signal events and 34.8 background events.

For $N_{TC} = 5$ the situation is improved considerably. The tensor peak is fully within reach of the 4 TeV machine, and the peak is more pronounced due to the $(N_{TC}/3)^{\frac{3}{2}}$ enhancement. See Figure 6. We find that the statistical significance of the signal is maximized with the cuts $M_{ZZ,T} > 2800$ GeV and $p_T > 180$ GeV, for which there are 221.9 signal events and 240.8 background events. The tensor peak for the case of $SU(5)_{TC}$ lies at ~ 2.6 TeV, so is partially visible at a 3 TeV $\sqrt{s_{e^+e^-}}$ collider, for which we find 46.3 signal events and 52.0 background events (relaxing the p_T cut slightly to 170 GeV).

4. Conclusions

In summary our conclusions are

- S/B for the nonresonant s-wave is small, even for $\sqrt{s_{e^+e^-}} = 4$ TeV.
- Significant signals are possible if there is a tensor resonance within the energy reach of the collider.
- The effect of fermionic cuts on the heavy Higgs signal should be investigated. We expect that the utility of this method is limited since the signal is falling rapidly and the background is growing rapidly at the limit of feasibility, $M_H \sim 400$ GeV. The Z bosons are less highly boosted so that the fermionic cuts are less efficient.
- Nonresonant strong scattering might be better observed in $\gamma\gamma \rightarrow WWW$ and $\gamma\gamma \rightarrow WWZZ$ [3].

5. Acknowledgements

MSC's work was supported by the Director, Office of Energy Research, Office of High Energy and Nuclear Physics, Division of High Energy Physics of the U.S. Department of Energy under Contract DE-AC03-76SF0. MSB's work was supported in part by the University of Wisconsin Research Committee with funds

granted by the Wisconsin Alumni Research Foundation, in part by the U.S. Department of Energy under contract no. DE-AC02-76ER00881, and in part by the Texas National Laboratory Research Commission under grant no. RGFY93-221 and by an SSC Fellowship.

6. References

1. I. Ginzburg, these proceedings, and V. Telnov, *op cit.*
2. M. Herrero and E. Ruiz-Morales, Phys. Lett. **B296**, 397 (1992); A. Abbasabadi, D. Bowser-Chao, D. A. Dicus, and W. W. Repko, Phys. Lett. **D49**, 547 (1994); J. F. Donoghue and T. Torma, Massachusetts Univ. preprint UMHEP-398, September, 1993; R. Rosenfeld, Northeastern University preprint, NUB-3074-93-TH, September, 1993; M. Baillargeon, G. Bélanger, and F. Boudjema, ENSLAPP-A-473/94, May, 1994.
3. S. J. Brodsky, talk presented at the 2nd International Workshop on Physics and Experiments with Linear e^+e^- Colliders, Waikoloa, HI, 26-30 Apr 1993; G. Jikia, these proceedings; K. Cheung, *op cit.* and Northwestern preprint NUHEP-TH-94-13, June, 1994.
4. M. S. Chanowitz and M. K. Gaillard, Nucl. Phys. **B261**, 379 (1985).
5. G. V. Jikia, Phys. Lett. **B298**, 224 (1992); Nucl. Phys. **B405**, 24 (1993).
6. M. S. Berger, Phys. Rev. **D48**, 5121 (1993).
7. B. Bajc, Phys. Rev. **D48**, 1903 (1993); D. A. Dicus and C. Kao, Phys. Rev. **D49**, 1265 (1994); H. Veltman, Saclay preprint SACLAY-SPHT-93-111, October, 1993.
8. M. S. Berger and M. S. Chanowitz, Phys. Lett. **B263**, 509 (1991); V. Barger, K. Cheung, T. Han, and R. J. N. Phillips, Phys. Rev. **D42**, 3052 (1990).
9. M. S. Chanowitz, M. Golden, and H. Georgi, Phys. Rev. Lett. **57**, 2344 (1986); Phys. Rev. **D36**, 1490 (1987).
10. J. F. Donoghue, B. R. Holstein, and Y. C. R. Lin, Phys. Rev. **D37**, 2423 (1988).
11. A. Dobado, J. R. Peláez, Z. Phys. **C57**, 501 (1993).
12. The Crystal Ball Collaboration, Phys. Rev. **D41**, 3324 (1990).

$\sqrt{s_{e^+e^-}}$	Polarization	Cross Section [fb]
1.5 TeV	Polarized	0.54
	Nonpolarized	0.34
2 TeV	Polarized	0.70
	Nonpolarized	0.52
3 TeV	Polarized	0.56
	Nonpolarized	0.65
4 TeV	Polarized	0.36
	Nonpolarized	0.59

Table 1: K Matrix Cross Sections without any cuts.

$\sqrt{s_{e^+e^-}}$	Polarization	Cross Section [fb]
1.5 TeV	Polarized	0.65
	Nonpolarized	0.38
2 TeV	Polarized	0.94
	Nonpolarized	0.65
3 TeV	Polarized	0.60
	Nonpolarized	0.77
4 TeV	Polarized	0.47
	Nonpolarized	0.72

Table 2: Linear Model Cross Sections without any cuts.

$\sqrt{s_{e^+e^-}}$	Model	M_{ZZT} Cut	p_T Cut	Signal S	Background B	Stat. Sig. S/\sqrt{B}
2 TeV	Linear	850	110	10.1	708.8	0.38
	K Unit.	800	90	8.3	866.6	0.28
3 TeV	Linear	900	110	11.9	781.9	0.42
	K Unit.	900	110	9.9	781.9	0.36
4 TeV	Linear	900	130	9.4	661.0	0.36
	K Unit.	900	130	7.8	661.0	0.30

Table 3: Event rates at unpolarized colliders with angle cut $\cos(\theta_{\text{lab}}) < 0.7$.

$\sqrt{s_{e^+e^-}}$	Model	M_{ZZT} Cut	p_T Cut	Signal S	Background B	Stat. Sig. S/\sqrt{B}
2 TeV	Linear	1050	120	18.8	907.4	0.62
	K Unit.	1050	110	14.0	961.8	0.45
3 TeV	Linear	750	140	11.9	823.4	0.41
	K Unit.	750	140	11.1	823.4	0.38
4 TeV	Linear	750	120	9.0	773.1	0.32
	K Unit.	650	110	6.6	817.4	0.23

Table 4: Event rates at polarized colliders with angle cut $\cos(\theta_{\text{lab}}) < 0.7$.

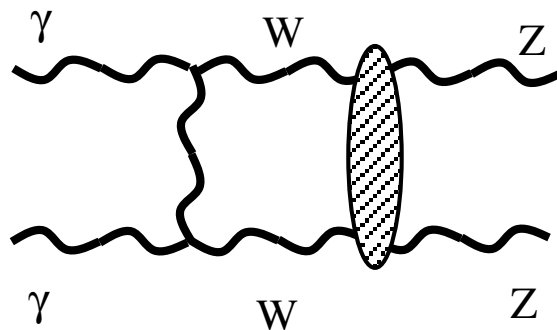


Fig. 1. The process $\gamma\gamma \rightarrow Z_L Z_L$ occurs via $\gamma\gamma \rightarrow W_L^+ W_L^-$ with a final state interaction by strong $W_L W_L$ scattering, as shown for example in the Feynman diagram above.

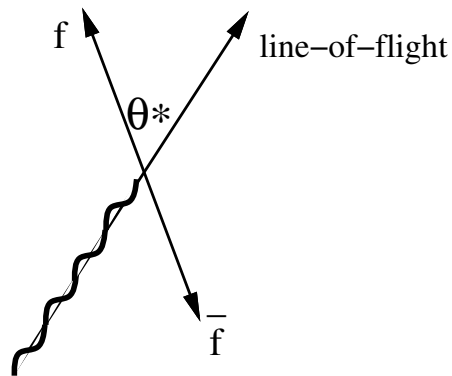


Fig. 2. The transversely polarized Z bosons tend to decay with one product along and one against the line-of-flight.

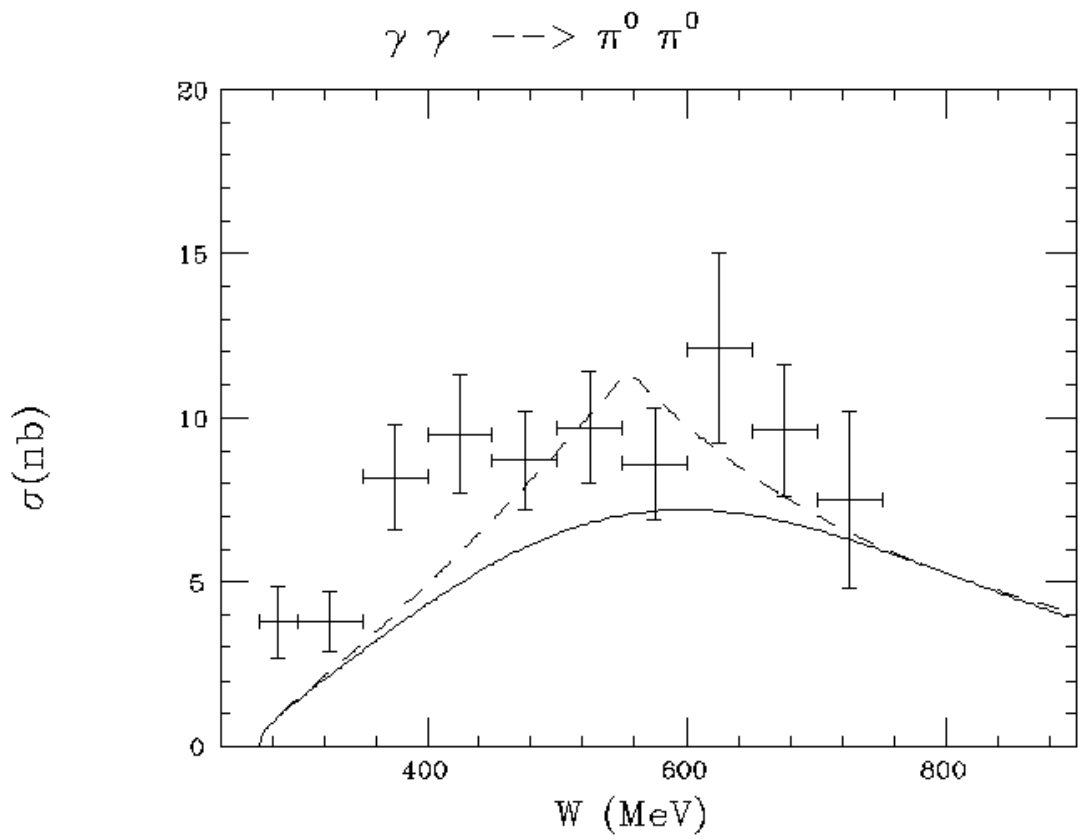


Fig. 3. The Crystal Ball data[12] with the linear (dashed) and K-matrix (solid) unitarized models for the $\gamma\gamma \rightarrow \pi^0\pi^0$ process ($W \equiv \sqrt{s}$).

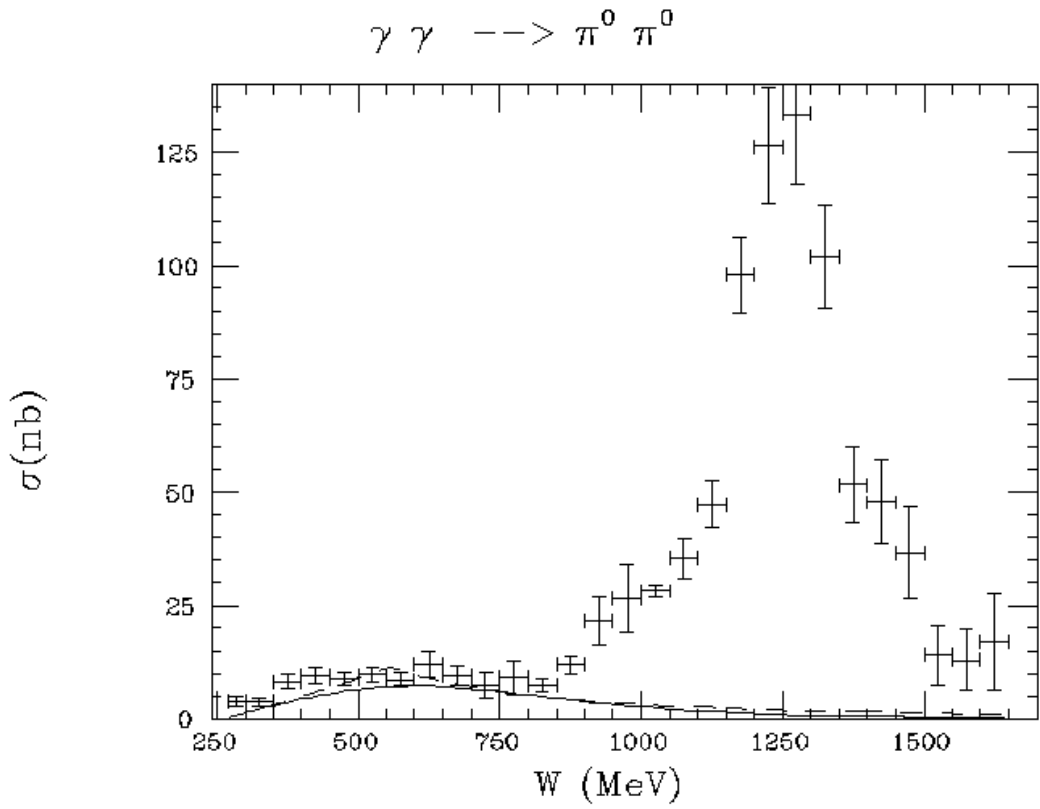


Fig. 4. The Crystal Ball data with the linear and K-matrix unitarized models for the $\gamma\gamma \rightarrow \pi^0\pi^0$ process. The tensor $f_2(1270)$ and the scalar $f_0(975)$ are visible ($W \equiv \sqrt{s}$).

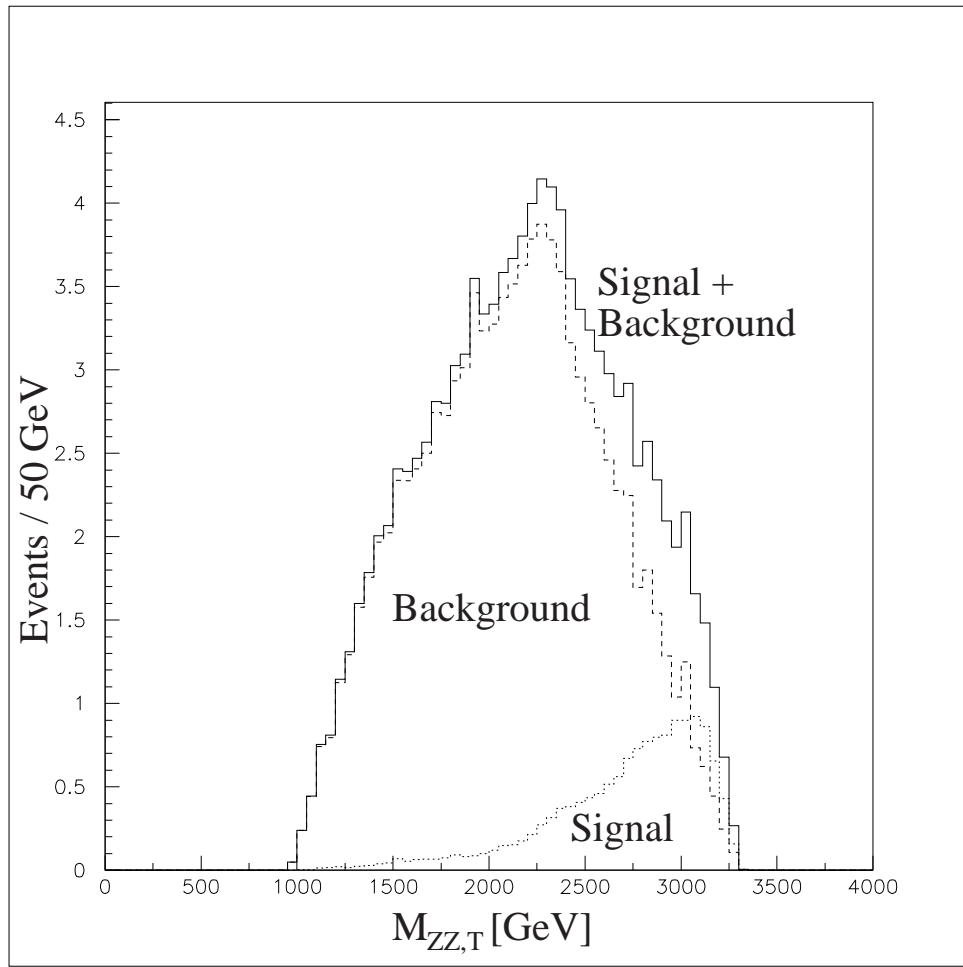


Fig. 5. The tensor contribution produces an enhancement over the purely s-wave contributions from the low-energy theorem. The signal and background are shown after the cuts $|\cos \theta_{\text{lab}}| < 0.7$ and $p_T > 240$ GeV for 10 fb^{-1} of integrated luminosity without including the branching ratios.

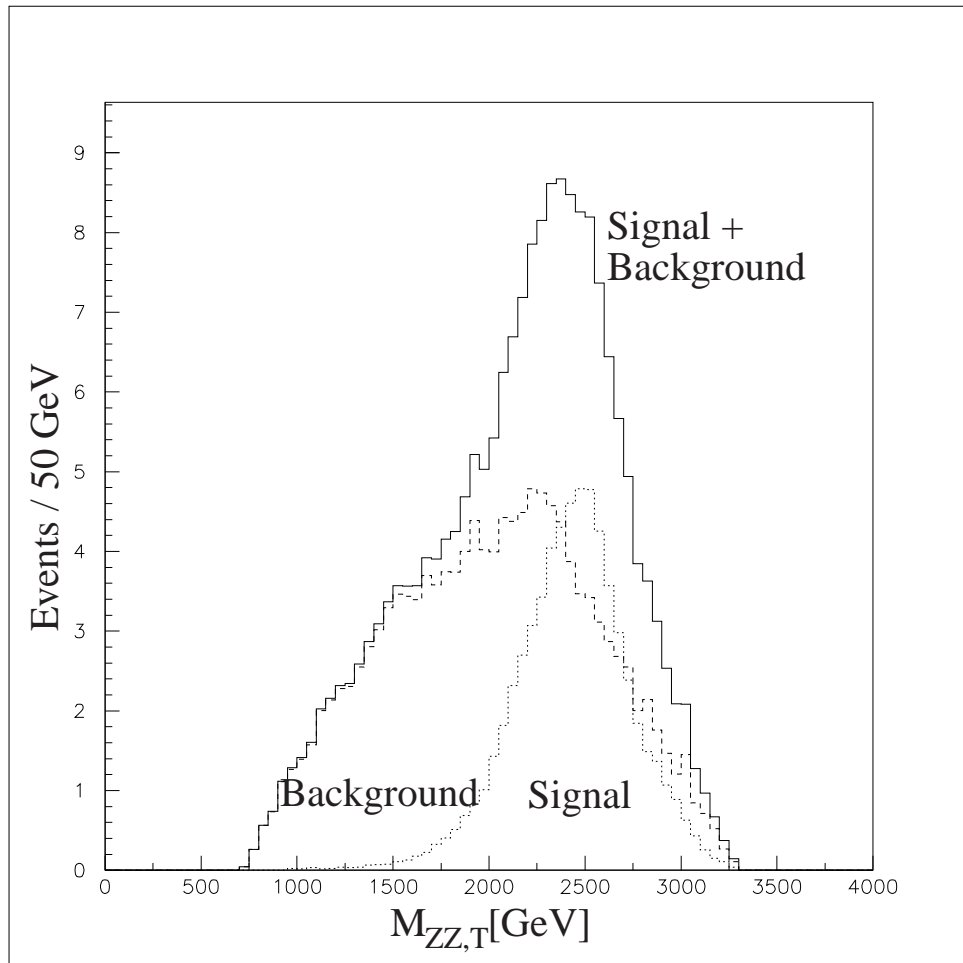


Fig. 6. The tensor contribution for $N_{TC} = 5$. The signal and background are shown after the cuts $|\cos \theta_{\text{lab}}| < 0.7$ and $p_T > 180$ GeV for 10 fb^{-1} of integrated luminosity without including the branching ratios.